

Copyright © 1975, by the author(s).  
All rights reserved.

Permission to make digital or hard copies of all or part of this work for personal or classroom use is granted without fee provided that copies are not made or distributed for profit or commercial advantage and that copies bear this notice and the full citation on the first page. To copy otherwise, to republish, to post on servers or to redistribute to lists, requires prior specific permission.

MULTIPLE-MIRROR PLASMA CONFINEMENT

Allan J. Lichtenberg, Michael A. Lieberman

and B. Grant Logan<sup>\*</sup>

Electronics Research Laboratory  
University of California, Berkeley, California 94720

Memorandum No. ERL-M541

September 22, 1975

ELECTRONICS RESEARCH LABORATORY  
College of Engineering  
University of California, Berkeley  
94720

## MULTIPLE-MIRROR PLASMA CONFINEMENT

Allan J. Lichtenberg, Michael A. Lieberman

and B. Grant Logan<sup>\*</sup>

Electronics Research Laboratory  
University of California, Berkeley, California 94720.

### ABSTRACT

A large enhancement of the confinement time can be achieved in a straight system of multiple mirrors over an equal length uniform magnetic field. The scaling is diffusive rather than that of flow, thereby scaling as the square of the system length rather than linear with system length. Probably the most economic mode of operation for a reactor occurs when  $\lambda/M \sim \ell_c$ , where  $\lambda$  is the mean free path,  $M$  the mirror ratio, and  $\ell_c$  the length between mirrors; but where the scale length of the mirror field  $\ell_m \ll \lambda$ . The axial confinement time has been calculated theoretically and numerically for all important parameter regimes, and confirmed experimentally. A typical reactor calculation gives  $Q_E = 2$  for a 400 meter system with 3000 MW(e) output.

The main concern of a multiple-mirror system is stability. Linked quadrupoles can achieve average minimum-B stabilization of flute modes, and experiments have demonstrated this stabilization. Localized instabilities at finite  $\beta$  and enhanced diffusion resulting from the distorted flux surfaces and possibly from turbulent higher order modes still remain to be investigated.

---

\* Present address - Lawrence Livermore Laboratory, Livermore, Ca. 94550  
This research was partially supported by ERDA Contract AT(04-3)-34 PA215  
and by National Science Foundation Grant ENG 75-02709.

## I. INTRODUCTION

A multiple-mirror device consists of a series of connected magnetic mirrors. In the appropriate plasma density and temperature regime for which the ion mean free path  $\lambda$  is much less than the device length  $L$ , but long compared to the scale length of the changing magnetic field  $\ell_m = B/(dB/dz)$ , repetitive trapping and detrapping of ions by the multiple mirrors leads to a diffusion loss process with the loss time scaling as  $L^2$ <sup>(1-8)</sup>. For  $\lambda > L$ , free flow exists for untrapped particles with loss on a time scale  $\tau \sim L/v$ , where  $v$  is the particle velocity, while trapped particles are lost by the usual scattering into the loss cone. For  $\lambda < \ell_m$  there is a gradual transition to MHD flow in which the loss time  $\tau \sim ML/v$  where  $M$  is the mirror ratio. This high density regime has an extended transition in which ion viscosity effects preserve the  $L^2$  diffusive scaling, although the full multiple-mirror confinement time is not realized.<sup>(4)</sup>

In the next section we show that the multiple mirror loss time is given approximately by  $\tau \approx \frac{M^2 L}{2\lambda} \frac{L}{v}$ . It is thus strongly enhanced over the free flow time if the mirror ratio is large and the mean free path is short. The mirror ratio is limited by magnetic field requirements and the requirement of  $\beta = p/(B^2/2\mu_0) < 1$ , where  $p$  is the plasma pressure and  $B^2/2\mu_0$  the magnetic pressure. The requirement that  $\lambda$  be small suggests that the temperature should be as low as possible and the density as high as possible, since  $\lambda \propto T^2/n$ . To see this more clearly we note that the power loss scales as  $P_\ell \propto nT/\tau_{mm}$ . Substituting for  $\tau_{mm}$ ,  $P_\ell \propto T^{3/2}/M^2 L^2$ . The fusion power, on the other hand scales as  $P_f \propto n^2 f(T)$ . For a reactor

the optimum T is approximately 4.5 keV for a D-T reaction. The density and the mirror ratio M are chosen as high as possible, limited by available magnetic field strengths at  $\beta < 1$ .

An alternative approach is to allow  $\beta > 1$  with the pressure taken up by a gas blanket and radial diffusion inhibited by the residual field. This approach is actively being pursued by the Novosibirsk group.<sup>(9)</sup> In the Novosibirsk high  $\beta$  configuration, as in a proposal by Tuck<sup>(10)</sup> for confinement of a  $\beta = 1$  plasma, the magnetic moment  $\mu$  is not conserved. However, another adiabatic invariant exists which acts similarly to the  $-\mu VB$  force to reflect particles. The reflections occur where the plasma diameter narrows due to the external mirror field. Tuck did not consider collisions, but rather discussed the possibility that the external field could be made to vary sufficiently fast that adiabaticity is lost, thus simulating the effect of fixed scattering center collisions. Other possibilities also exist for decoupling  $\lambda$  from  $n$  by introducing non-adiabatic components in the external field.<sup>(11)</sup> It has also been found that improved total performance can be achieved by seeding the plasma with a small percentage of high Z material.<sup>(12)</sup>

The multiple-mirror device can be incorporated into a number of reactor concepts. As a steady-state reactor the entire device can consist of mirrors in which case the density drops continuously from the center of the device to the ends. Alternatively, a constant central magnetic field region can be end-stoppered with multiple mirror sections. In this case the scaling is not as favorable, but the power distribution is improved. The multiple-mirror configuration can also be used with a two-component reactor.<sup>(12)</sup> In fact, studies show that some form of end stoppering is

required with a two component plasma to reduce the length required to contain the cold component.<sup>(12)</sup> In a steady-state reactor, plasma heating for start-up or energy injection for operation below the self sustaining length might be accomplished by intense electron beams, or naturally, in the two component concept, by neutral injection. A pulsed linear  $\theta$ -pinch reactor may also be stoppered, in principle, with multiple-mirror end sections, but details of a reactor configuration of this type, including stabilization for the mirror sections, have not been explored.

A typical steady-state reactor calculation gives the following results.<sup>(7)</sup> Assuming an upper limit of 200 kG for superconducting coils, with peak mirror fields of 300 kG provided by small conventional coils, typical reactor parameters are: length  $L = 400$  m and density  $n = 8 \times 10^{10} \text{ cm}^{-3}$  with net electrical power output  $P(\text{net}) = P(\text{recirculating})$ . For  $P(\text{net}) = 3000$  MWe, the plasma diameter is 3 cm. To improve the power distribution, the mirrors are placed only at the ends of the system, there being 20 cells, each 5 m long, at each end. The breakeven reactor would be 140 m long, and the self-sustaining condition  $P(\text{recirculating}) = 0$  occurs at  $L = 1100$  m.

In common with toroidal devices, multiple-mirror containment is at best average minimum  $B$ , and therefore subject to localized modes.<sup>(13)</sup> At high  $\beta$ , the connection lengths for localized mode suppression are small, but reactor designs can conveniently minimize the connection length. Drift instabilities would be expected to enhance radial diffusion, which can be serious in these naturally small diameter systems. If linked quadrupole stabilization is used the field line fanning will also enhance radial diffusion. These problems must all be considered carefully in

evaluating the multiple-mirror concept. Because the loss cone is nearly full, the multiple mirror should not be subject to velocity space instabilities.

In Sec. II we will review the theory of multiple-mirror confinement, and the results of computations. Reactor calculations will be given in Sec. III. In Sec. IV the results of experiments confirming the multiple mirror scaling laws will be reviewed. In Sec. V experiments using average minimum-B stabilization will be presented.

## II. THEORY

Consider a symmetric multiple-mirror system with  $F$  particles per unit area per unit time injected into the center in the steady state. The mirror widths  $\ell_m = B(dB/dz)^{-1}$  are assumed to be small compared to  $\ell_c$ , so that the loss cone angle  $\theta_c$  defined by

$$\sin^2 \theta_c = \frac{1}{M}, \quad (1)$$

where  $M \equiv B_{\max}/B_{\min}$  is the mirror ratio, is a constant over the cell length  $\ell_c$ . For many cells ( $L \gg \ell_c$ ) large mirror ratios ( $M \gg 1$ ), and sufficient source strength  $F$  such that the scattering mfp  $\lambda \ll L$ , particles will be trapped and untrapped many times before reaching the ends, so that their axial motion can be described by a random walk.

Since the distribution of velocities in such a system may approach a Maxwellian, the scattering distances for individual particles vary from distances much less than  $\ell_c$  to distances much greater than  $\ell_c$ . Considering the velocity groups which would have average step length  $\ell_z$

much greater than  $\ell_c$  (but  $\ell_z$  still  $\ll L$ ), the average step length  $\ell_z$  and step time  $t$  can be estimated from average times  $t_1$  and  $t_2$  spent out and in the loss cone respectively. For particles at speed  $v$ , and  $M \gg 1$  (small  $\theta_c$ ) we can estimate

$$t_2(v) \approx \tau_\theta(v) \theta_c^2 \approx \tau_\theta(v)/M, \quad (2)$$

where  $\tau_\theta(v)$  is the scattering time at speed  $v$  for a mean-square deflection of  $\theta = 1$  radian. We define the average step length between successive trappings. to be

$$\ell_z(v) \equiv \alpha t_2(v) v \approx \lambda/M \quad (3)$$

where  $\alpha$  is a proportionality constant of the order of unity which can be determined by a more exact theory or by experiments.

Assuming the velocity-space density of ions at speed  $v$  in the loss cone is nearly the same as that out of the loss cone, (e.g. a Maxwellian) statistical mechanics gives the ratio of trapped time  $t_1(v)$  to untrapped time  $t_2(v)$ <sup>(1)</sup> equal to the ratio of trapped to untrapped surface area at radius  $v$  in velocity space:

$$\frac{t_1(v)}{t_2(v)} = \frac{\cos \theta_c}{1 - \cos \theta_c} \approx 2M \quad (M \gg 1) \quad (4)$$

Equation (4) was found to qualitatively describe numerical results for  $t_1/t_2$ <sup>(1)</sup>. For large  $M$ ,  $t_2(v)$  can be neglected compared to  $t_1(v)$  in the total step time  $t(v) = t_1(v) + t_2(v)$ , and Eq. (4) with Eq. (3) gives  $t(v) \approx 2\tau_\theta(v)$ . Note that for  $\alpha$  of order unity and  $\ell_z(v) \gg \ell_c$ ,  $t_1$  is



many bounce periods  $\ell_c/v$ , so that the concept of trapping is well defined.

We define a diffusion coefficient for the velocity group  $v$  satisfying

$\ell_z(v) \gg \ell_c$  as

$$D(v) \equiv \frac{\ell_z^2(v)}{2t(v)} = \frac{\alpha \ell_z(v) v}{4M} \quad (5)$$

If this limit holds for most particles in all cells, the averaging over velocity gives  $\bar{D} \sim \frac{1}{n}$ , and integration of  $-\bar{D} \nabla n = \frac{F}{2}$  gives an exponential density profile:

$$n(z) = n_1 \exp\left[-\frac{Fz}{\bar{D}_a n_a}\right] \quad (6)$$

where  $\bar{D}_a$  is given by Eq. (5) evaluated at the average density  $n_a$ . The containment time is

$$\tau_{mn} = \frac{n_a L}{F} \frac{L^2}{\bar{D}_a} [\ln(n_1/n(L))]^{-1} \quad (7)$$

where  $n_r$  is the density in the center cell.

Alternatively for  $\ell_z/\ell_c \ll 1$  the cell length  $\ell_c$  is the basic step size and a straightforward analysis yields<sup>(7)</sup>

$$D_{\min}(v) = \frac{\ell_c v}{4M} \quad (8)$$

where the subscript min refers to the minimum diffusion coefficient at a fixed  $\ell_c$ . If this relationship holds for most particles in all cells,

then the density profile is triangular;  $dn/dz = \text{const.} \equiv n_1(L/2)$ , with an average density  $n_a = \frac{1}{2} n_1$ . For a discrete system of  $N = L/2\ell_c$  cells in a half length  $L/2$ ; the maximum density  $n_1$  in the center cell is given by

$$n_1 = N \Delta n, \quad (9)$$

where  $\Delta n$  is the density increment across each mirror. The containment time for this case is

$$\tau_{\text{mm}} (\text{max}) = \frac{\frac{1}{2} n_1 L}{2 \bar{D}_{\text{min}} \nabla n} = \frac{L^2}{8 \bar{D}_{\text{min}}} = \frac{ML^2}{2\ell_c \bar{v}} \quad (10)$$

A number of theoretical treatments have been devised, valid for both of these limits, as well as for the transition between them, giving essentially the results indicated here. (4), (6) In addition to calculations of the particle flux  $F = -D\nabla n$ , the end loss energy flux

$$G = - \frac{\int_0^{\infty} \left(\frac{1}{2}mv^2\right) D(v) \nabla n f_0 4\pi v^2 dv}{\int_0^{\infty} f_0 4\pi v^2 dv} \quad (11)$$

can also be calculated. Defining  $\lambda^* \equiv \bar{\lambda}/M$ , if we take the product  $(G/kTF)(\bar{D}_{\text{min}}/\bar{D})$  to obtain the relative variation of  $G$  as a function of  $\lambda^*/\ell_c$  we find that the product has a broad flat region near  $\lambda^*/\ell_c = 1$ , rising slowly for  $\lambda^*/\ell_c < 0.2$  and falling slowly for  $\lambda^*/\ell_c > 5$ . Considering that the system length  $L$  and the density, and therefore  $\lambda^*$ , are held fixed, we obtain the result that the energy flux decreases slowly, i.e., the energy confinement time increases slowly with increasing number of mirrors. The limiting case is the corrugated magnetic field structure.<sup>3,4</sup>

For economy of design, long mirrors are desirable, and we therefore will concentrate our attention on the region for which  $\lambda^*/\ell_c \approx 1$ .

The high density regime needs to be looked at separately, however, for if  $\lambda \ll \ell_c$  then it is also likely that  $\lambda < \ell_m$ . In this case the magnetic moment is not constant in the mirror region and the ion flow is limited by ion viscosity. For  $M \gg 1$  and  $\ell_m \ll \ell_c$  Mirnov and Ryutov<sup>(4)</sup> obtain

$$\tau = \frac{M \ln(M)}{2\ell_c v} \frac{\lambda}{\ell_m} \quad (12)$$

Thus the confinement time is reduced proportional to  $\lambda$  as MHD flow is approached. In an unpublished calculation, Berk, leaving the magnitude of  $M$  arbitrary, has found in the dominant diffusion term  $\tau \propto (M-1)^2$  so that multiple mirror confinement also ceases, as expected, at  $M = 1$ .

Numerical calculations of containment time in a multiple mirror device were made using a model in which the field particle densities, drift velocities and temperatures are included in a self consistent manner.<sup>(6)</sup> A number of test particles are numerically followed through the multiple mirror system with the velocity vector of each test particle varied on each step. The variation is composed of two parts, an adiabatic change due to the variation of the magnetic field and a random change arising from small angle coulomb collisions with the background plasma. The random small angle scattering is computed in the center of mass frame of the background plasma which is drifting, and the velocity vector transformed to the laboratory frame for computation of the adiabatic motion. The mathematical procedure is presented in Ref. (1) and (6). The confinement times of a large number of test particles are averaged

to obtain a multiple mirror confinement time. The mirror regions were peaked in accordance with the theory and also to simulate actual reactor designs. The results confirmed both the  $L^2$  scaling and the value of the containment time predicted from the theory with  $\lambda^* \approx \ell_c$  at the average density. (6)

In the preceding analysis, one important factor that has not been taken into account is the electrons. The electrons diffuse more rapidly than the ions by the ratio  $(M/m)^{1/2}$  and thus are contained by an ambipolar force required to preserve charge neutrality. As the electrons are in thermal equilibrium with the ions they increase the axial diffusion by a factor of two. Heat conduction must also be considered. This is rapid compared to the ion containment time within the multiple-mirror system and therefore keeps the temperature constant. At the machine ends care must be taken that cold electrons are not available to re-enter the device exchanging energy with the hot trapped electrons. This problem, common to mirror devices, is generally thought to be accomplished by expansion of the field lines, which would be required, anyway, if direct conversion is employed. Although there is considerably higher density in multiple-mirror devices than in single mirrors, the density in the end cells of the multiple mirror is approximately  $1/N$  smaller than that of the central cells.

### III. REACTOR CALCULATION

A preliminary evaluation of the significance of the multiple mirror concept has been made by estimating parameters for a steady state reactor (assuming no anomalous radial loss). We have the following energy flows associated with a DT multiple-mirror fusion reactor of length  $L$ : fusion neutrons  $P_n$ , fusion alphas  $P_\alpha$ , bremsstrahlung power loss  $P_\beta$ , and power

loss associated with plasma loss along field lines  $P_\ell$ . Taking a practical magnetic field limit  $B_{\max}$  in all mirror throats, the midplane field is chosen to maintain the plasma beta constant, which allows for the maximum mirror ratio in each cell. The density profile is calculated from diffusion theory to be  $n(z) \approx n_1 [1-z/\chi]^{3/2}$  and the temperature profile is uniform, where  $z$  measures the distance along the density gradient region of length  $\chi$  (allowing  $\chi < L/2$ ) and the subscript 1 refers to the center cell. The cell length  $\ell_c$  is chosen to be  $\ell_c = 4 \lambda_1 / M_1$ . The details of this calculation are given in Ref. 7.

We assume  $P_n$  and  $P_\beta$  are converted into electricity by a thermal cycle at efficiency  $\eta_T$ ,  $P_\alpha$  is deposited directly within the plasma, and  $P_\ell$  is directly converted into electricity at efficiency  $\eta_{DC}$ . The power ratio  $Q_E$  is defined as

$$Q_E \equiv \frac{P(\text{total electrical power generated})}{P(\text{injected, or recirculating electrical power})}$$

For  $P_{\text{net}} \geq 0$ ,  $Q_E \geq 1$ . We choose a trapezoidal density profile such that the multiple mirrors are acting as stoppers for a constant density central section.  $Q_E$  can be optimized with respect to the axial profile for fixed  $L$ , and the results indicate a broad maximum with equal uniform and multiple-mirror sections but with substantially improved power distribution. Using this distribution we minimize  $L$  with respect to  $T$ . For  $Q_E = 2$ ,  $T = 4.5$  keV; for  $Q_E = \infty$ , corresponding to the self sustaining condition  $P_\alpha = P_\ell + P_\beta$ ,  $T = 6$  keV.

The maximum density  $n_1$  is set by limits on  $B_{\min}$  in the central region of the reactor, and by the plasma beta. Assuming  $B_{\min} = 200$  kG,  $\beta = 0.8$  and  $B_{\max} = 300$  kG, an internal mirror ratio  $M \approx 2.7$  is then created at

$n = n_1$ . Using  $\eta_T = .5$  and  $\eta_{DC} = .75$ ,  $Q_E$  is plotted as a function of  $L$  in Fig. 1. The minimum length for economic operation is probably  $L = 400$  meters, which corresponds to  $Q_E = 2$ . At that point the parameters of interest are  $T_e = T_i = 4.5$  keV,  $n_1 = 8 \times 10^{16} \text{ cm}^{-3}$ ,  $\lambda(n_1) = 3.3$  meters,  $\ell_c = 5.0$  meters (20 cells on each side in the density gradient regions), and  $\tau_{\text{mm}} \approx 30$  millisecc. A plasma diameter of 3 cm would be required to produce 10 MW(e) net per meter at  $T = 4.5$  keV, which at  $Q_E = 2$  would produce 3000 MWe net power. Further details of this calculation are given in Ref. 7.

One possible method of supplying the recirculating energy is by high energy neutral injection transverse to the device. An additional benefit is the power produced by hot deuteron-warm triton fusion reactions. Computational studies of energy balance in such a two component reactor have been undertaken to investigate if better reactor parameters are available under two-component operation. A simplified reactor was considered in which equal length mirrors were placed along the entire length of the device, and in which direct conversion of charged particle energy was not employed. The energy flows between the hot and warm components and the thermal converter are shown in Fig. 2. The hot component is non-Maxwellian with density  $n_h$ , and is supplied by an energetic neutral deuterium beam with beam energy  $E_0$ . The warm component is Maxwellian at temperature  $T$ , consisting of a density  $n_d$  of deuterium and  $n_t$  of tritium. The total ion density  $n_i = n_h + n_d + n_t$ . As shown in the figure, of the injected beam power density  $P_{\text{inj}}$ , a power density  $P_t$  is collisionally transferred to the warm component, with a small scattering loss  $P_s$  remaining. The energy loss of the warm component is by bremsstrahlung  $P_\beta$  and multiple mirror loss  $P_\ell$ . Fusion reactions between both hot and warm

deuterons, and warm tritons, produce neutron power densities  $P_{nh}$ ,  $P_{nw}$  and alpha particle power densities  $P_{\alpha h}$ ,  $P_{\alpha w}$  respectively. The alpha particles deposit their entire energy in the warm plasma.

The distribution of the hot component is obtained from the Fokker-Planck equation, and the power densities  $P_s$ ,  $P_t$ ,  $P_{nh}$  and  $P_{\alpha h}$  are then evaluated. These power densities, along with  $P_{nw}$ ,  $P_{\alpha w}$  and  $P_\beta$  all scale proportional to  $n_e^2$ , independent of the reactor length  $L$ . On the other hand, the multiple mirror loss  $P_\ell$  is proportional to  $T^{7/2}/L^2$ , independent of  $n_e$ . The equation for power balance in the warm plasma

is

$$P_t + P_{\alpha h} + P_{\alpha w} - P_\beta = P_\ell, \quad (13)$$

which can be cast in the form

$$\frac{1}{pL^2} = X(E_o, T, f, \epsilon, M), \quad (14)$$

where  $f = n_d/(n_d+n_t)$ ,  $\epsilon = n_h/n_e$ ,  $M$  is the mirror ratio, and the plasma pressure  $p \propto n_e$  has been used. Thus if the plasma pressure  $p$  is doubled, the reactor length is halved.

To optimize the system, we write

$$Q = (P_{\text{fusion}} + P_{\text{inj}})/P_{\text{inj}} \quad (15)$$

$$= Q(E_o, T, f, \epsilon, M),$$

where  $P_{\text{fusion}}$  is the total thermal fusion power density. Holding  $Q$  fixed, we maximize  $X$ .

For a given  $E_o$ ,  $T$  and  $M$ , optimum values of  $f$  and  $\epsilon$  are then determined. For these values, a minimum reactor length is found. The results are

presented in the form of contours of constant length  $L$  and the corresponding  $f$ , on a  $T$ - $E_0$  diagram, for fixed  $Q$  and  $M$ . A typical result is shown in Fig. 3, for  $Q = 3$  and  $M = 3.3$ . For these values, the minimum length system occurs for  $T \sim 4.7$  keV,  $E_0 \sim 190$  keV. At  $T = 5$  keV,  $E_0 \sim 180$  keV, and  $p = 900$  atm,  $L \sim 430$  m,  $n_e \sim 6 \times 10^{16} \text{ cm}^{-3}$ ,  $f = .39$ ,  $\epsilon = .0015$ , the reactor consists of 78 equally spaced cells, and the energy confinement time is 4 ms. For  $P_{\text{fusion}} + P_{\text{inj}} = 5000$  MW, the plasma diameter is 4 cm, and the injected beam current is 9 kA. For a pure multiple mirror ( $f = 0.5$ ) with  $Q = 3$  and the injected power supplied by means other than a fast neutral beam, the corresponding reactor length is 530 m.

Studies for various values of  $Q$  and  $M$  have been compared with the results from a pure two component system ( $f \equiv 0$ ). For  $Q$  less than about 2.5, the  $f = 0$  solution (warm plasma pure tritium) produces the smallest length. For  $Q > 2.5$ , the minimum length system has  $f > 0$ , with  $f \rightarrow 0.5$  as  $Q \rightarrow \infty$  which is the self-sustaining condition. For comparison with the above length, the result for  $f = 0$  at  $Q = 3$  is  $L = 513$  m.

Another study involves the addition of a small fraction  $f_z$  of a fully ionized, low  $Z$  impurity to the warm plasma. This impurity produces effects in the power balance equation which are proportional to  $Z^2 f_z$ ,  $Z f_z$  and  $f_z$ . In addition, there are power flows due to free-bound and bound-bound bremsstrahlung if the impurities are not fully ionized. The dominant effects are those which scale as  $Z^2 f_z$ . These include: (1) an increase in free-free bremsstrahlung radiation  $P_\beta$ ; (2) a reduction in multiple mirror power loss  $P_\lambda$ , due to increased scattering of warm D and T ions against the impurity ions; and (3) an increase in  $P_s$  due to



hot ion scattering against impurity ions. If the reduction in  $P_\ell$  is greater than the increase in  $P_\beta$  and  $P_s$ , then the addition of impurities will cause the reactor length to decrease.

A code has been developed to minimize the system length, including all these terms. Typical results are shown in Fig. 4. It can be seen that there is a reduction in system length of order 10%. Perhaps of more significance, multiple mirror operation is possible at considerably higher temperatures than are possible in the absence of impurities. This is of importance because in the absence of impurities D and T ions in the extreme Maxwellian tail of the warm component generate the bulk of the fusion power.

Another possible energy injection method employs an axial electron beam. For example with injection at 100 keV, one would require  $3.10^4$  amperes of electrons steady state. It has been shown that, even in the absence of strong collective effects, a 100 keV electron beam will collisionally transfer most of the energy along a plasma column of the density and length of the proposed reactor.<sup>(14)</sup> Studies of energy absorption for MeV beams in multiple mirrors are being pursued, among other places, at Physics International,<sup>(15)</sup> and at Novosibirsk.<sup>(9)</sup>

In a driven steady state system, the plasma energy loss must be replenished by injection. On the other hand, in a pulsed multiple mirror reactor using a theta-pinch to form the plasma, the plasma energy can be supplied during startup by shock heating followed by adiabatic compression.<sup>(16)</sup> Little study of this concept has been undertaken in the context of multiple-mirror reactor design.

#### IV. AXIAL CONFINEMENT EXPERIMENTS

Because the mean free path scales as  $\lambda \propto T^2/n$  it is possible to scale laboratory size experiments over a wide range of temperatures and densities while maintaining  $\lambda \sim \ell_c$ . A convenient steady state plasma can be created with a "Q-machine" source. Experiments with this type of source have been carried out at Berkeley<sup>(5,7)</sup> and at Novosibirsk.<sup>(8)</sup> The steady-state plasma generated at a hot plate simulates a central source for a multiple mirror device, with the length of the experimental system being one-half of a symmetrical device. Simple magnetic mirrors can be used in this configuration, as the plasma is stabilized by line-tying to the hot plate. The effects of neutrals can be made negligible, but recombination at the hot plate, as well as radial loss, must be considered.

The Berkeley Multiple Mirror Device (Fig. 5) contained a series of water-cooled coils forming up to 8 mirror cells along a 6 cm. dia. 150 cm long vacuum chamber. The peak magnetic field is in the 5 kG range and the mirror ratios could be varied between 1 (nearly uniform) and a large number (say 10) depending on the coil configuration. The plasma length was varied by moving a negatively biased collector plate along the chamber axis, as shown in Fig. 5. The end loss rate of ions was measured by the collector current  $I_c$ . The number of mirror cells  $N = L'/\ell_c$  was varied either by moving the collector within a fixed multiple-mirror field, or by switching mirrors on and off between the source and a fixed collector. The plasma density was measured by Langmuir probes which could be moved both radially and longitudinally to explore the entire plasma volume. A comprehensive set of experiments have been performed confirming the variation of confinement time with the square of number of cells and the

predicted variation with average mirror ratio. The stepwise density fall-off from cell to cell, and the stepwise increase in density in the first cell as new cells were added, was also demonstrated. The experimentally determined values of the confinement time were also in reasonable agreement with those expected from the theory. The transition to the free flow regime at low density and to the MHD flow regime at high density were also demonstrated. (7)

Here we give examples from some of these results. In Fig. 6, we compare the density profile for a long mirror with a three cell system of the same overall length. Figure 6a shows the density profile at low density indicating the free flow behavior in which the density follows the magnetic field variation. In Fig. 6b, the density has been increased to the intermediate mean free path regime in which the increased density in the first cell and the characteristic stairstep density pattern is observed. The ratio of confinement times of 2, between the multiple-mirror and the long-mirror configurations is as predicted by the theory.

Another test of the scaling law of multiple mirror confinement time with the number of mirror cells can be made by observing the changes in the density in the first cell,  $n_1$ , for a constant source, as the collector is withdrawn within a fixed multiple mirror field, thus adding mirror cells to the system. Figure 7 shows the probe current ( $\propto$  density) in the first cell next to the source as a function of collector position in the (a) low, (b) intermediate, and (c) high density regimes. In Fig. 7 the density at the source is seen to increase in a stepwise fashion as

the collector passes each mirror throat, adding another cell to the system. The increase in density is strongest in the intermediate density regime, as expected. The first density jump, corresponding to the collector passing the second mirror, is a result of partial filling of velocity space due to ion trapping when the first cell is created, and is not a multiple-mirror effect.

The Novosibirsk device<sup>(8)</sup> had 13 mirrors over a 2 meter length and could be switched between a uniform field and a mirror ratio of  $M = 1.83$  with  $B_{\text{Max}} = 5,400$  Gauss. The device operated in a density range for which  $\lambda^* > \lambda_c$  such that the axial density distribution should vary exponentially. Comparison of the density in the last cell,  $n_L$ , with the density in a cell, nine cells closer to the source,  $n_9$ , gave increasing ratios of  $n_9/n_L$  as the density was increased, indicating the gradual transition from the free flow to the multiple mirror regime. At the highest density of stable operation they obtain  $n_9/n_L \approx 4$ , which was in good agreement with the theoretical value of  $n_9/n_L = 9/(2 \ln 9)^{1/2} = 4.3$ . Switching to a uniform field gave  $n_9/n_L \approx 1$ , as expected. They also operated in a transient (but still line-tied) mode by intercepting the neutral flux before it reached the hot plate. The increase in the transient plasma lifetime with increase in plasma density was consistent with that expected from increasing multiple mirror action.

## V. STABILITY CONSIDERATIONS

The primary problems connected with the multiple-mirror reactor concept at  $\beta < 1$  are radial stability and diffusion. A magnetic configuration consisting of magnetic mirrors and linked quadrupole fields can make a

weak average minimum-B well on the axis.<sup>(17)</sup> Calculations are continuing at Berkeley, to determine the optimum configuration of magnetic fields with practical coil designs. One limitation of this type of stabilization is the onset of localized modes with finite  $\beta$ . A criterion for stability against these modes is<sup>(13)</sup>

$$\beta_c \approx \frac{8\pi^2 \gamma r_p R_c}{L^2}, \quad (16)$$

where  $\gamma$  is a ratio of average good curvature to the characteristic curvature  $R_c$ ,  $r_p$  is the plasma scale length and  $L$  the connection length. Although it is difficult to calculate these quantities outside of a specific design, we estimate that  $\gamma \approx 1/10$ ,  $r_p R_c / L^2 \approx 1/10$  such that  $\beta \approx 1$ . We expect, therefore, that substantial  $\beta$ 's are possible in realistic reactor geometries.

In addition to the above limitations, ave. min.-B stabilization will increase radial diffusion, due to the distortion of the magnetic surfaces. Previous estimates indicated that for an azimuthally symmetric plasma at  $\beta = .8$ , a perpendicular diffusion coefficient of  $D_{\perp} = 10^{-3} D_{\text{Bohm}}$  could be tolerated. This requirement becomes somewhat more stringent if the plasma is fanned. In addition, practical considerations, such as coil design, become less straightforward.

Other methods of stabilization not requiring distorted magnetic surfaces, may be possible, and should be investigated further. Among these we mention line-tying, wall current stabilization, and feedback stabilization. The same line-tying mechanism by which the "Q-machine" plasmas are stabilized can, at least in principle, be applied to plasmas at higher density and temperature. The key questions are how large a supply of

electrons need to be available for stabilization, and whether this level of electron injection will unacceptably increase the axial heat conductivity. Theoretical and experimental investigations of these questions are currently in progress at Berkeley.

An initial analysis of wall current stabilization indicates that the method can be effective in suppressing flutes. Alternating the stabilization current can prevent the appearance of current driven modes. A calculation for reactor parameters indicated stabilization with an oscillating current of 5kA, well below the random current.<sup>(18)</sup> Comparison of currents with a long thin mirror system with the dynamic stabilization currents needed in Syllac show that this current is an order of magnitude less than would be required to dynamically stabilize a toroidal device<sup>(19)</sup>. The requirement of having a close wall may be a difficulty with this scheme. The stabilization scales in such a manner that it is difficult to test the method on a small experiment. The small radius of a multiple mirror plasma indicates that few modes would be present, and therefore opens the possibility of feedback stabilization. Multi-mode stabilization has been carried out at Berkeley,<sup>(20)</sup> and is actively being considered as a possible stabilization mechanism for a larger multiple-mirror device.

The Berkeley multiple-mirror experiment has been modified to include linked quadrupole fields, for average minimum-B stabilization. The basic design follows principles described in an article by Furth and Rosenbluth.<sup>(17)</sup> Practical constraints of coil size, mirror lengths, and external leads, altered the design shape sufficiently that average min-B could not be attained. Subsidiary trim coils (arc straps) designed to counteract the adverse effects of the leads, which weaken B where the curvature is un-

favorable, did not fully counteract these adverse effects. In the final design the unfavorable average curvature was improved by a factor of 2 at one half centimeter radius in the compensated system. The shape of characteristic field lines at the optimum design parameters is given in Fig. 8. The ellipticity is approximately 10 in this design. The corresponding magnet and quadrupole configuration is given in Fig. 9.

Transient experiments, to test both confinement and stability, have been performed in two density and temperature ranges.<sup>(21)</sup> In the first, a gating coil creates a cusp field between the multiple mirrors and the hot plate to eliminate both the source of new plasma and the line tying. Without the quadrupole fields the plasma becomes flute unstable and moves transversely to the walls. Despite the lack of complete compensation, there is a narrow range of parameters in which at least partial stabilization can be obtained. In Fig. 10, the decay time in msec is plotted against the ratio of quadrupole to mirror current. The onset of stabilization, for this set of parameters, is clear. The longest decay time of 0.7 msec can be compared with the theoretically optimum decay of 4 msec, or with an estimate of the actual expected decay (non optimum) in this transient situation of about 1.5 msec.

In the second experiment a higher density and temperature transient plasma was created by a conical  $\theta$ -pinch source. Keeping  $\lambda \propto T^2/n$  constant, the temperature was scaled up by a maximum of two orders of magnitude to  $T \approx 20$  eV, and the density scaled correspondingly by  $10^4$ , to  $n \approx 10^{14}$ . This temperature range with a density of  $10^{15}$  (required to allow for expansion into the multiple-mirror) was achieved with a 50 kV, 2  $\mu$ f capacitor at a filling pressure of  $\sim 20$  Torr of hydrogen. The gas fill

is accomplished with a pulsed gas valve to keep the main system at low pressure, with a 50 cm uniform magnetic guide field used to separate the neutrals by time-of-flight (400  $\mu$ sec) from the experiment which has a characteristic decay time of about 100  $\mu$ sec. An additional fast gating coil can be used to prevent the influx of slower plasma. The experimental results were similar to those at low temperature and density, showing an onset of stabilization with increasing quadrupole current. Axial profiles of the density at successive times for the uncompensated and compensated decay are shown in Fig. 11. The stabilized decay obtained was 70-90  $\mu$ sec as compared to the theoretical optimum of 200-300  $\mu$ sec and the expected decay of a stable plasma of 100-150  $\mu$ sec. The uncertainty in the theoretical calculation of the decay is due mainly to an uncertainty in the ion temperature, which is falling during the experiment. There is a characteristic self compensation in this type of transient experiment that tends to maintain the correct mean free path; the hot particles scatter out preferentially, cooling the plasma as the density decays.

A number of reasons may be advanced for the improvement of stability over that predicted from MHD theory. Although finite Larmor radius effects theoretically do not stabilize the  $m = 1$  mode in azimuthally symmetric systems, they may have an effect in the strongly fanned configuration, particularly as the stabilization was more pronounced in the hotter plasma in which there are only two to three Larmor radii across the narrow dimension of the ellipse. A related stabilizing effect from non-uniform plasma rotation could arise from ambipolar electric fields. Residual line tying could also play a role, as it was observed that, although little plasma was injected from the  $\theta$ -pinch source late in the decay,



considerably better stabilization was achieved when the fast gating coil was not activated in the experiment.

## VI. CONCLUSION

A large enhancement of the confinement time can be achieved in a straight system of multiple mirrors over an equal length uniform magnetic field. The scaling is diffusive rather than that of flow, thereby scaling as the square of the system length rather than linear with system length. Probably the most economic mode of operation for a reactor occurs when  $\lambda/M \sim \ell_c$ , where  $\lambda$  is the mean free path,  $M$  the mirror ratio, and  $\ell_c$  the length between mirrors; but where the scale length of the mirror field  $\ell_m \ll \lambda$ . The axial confinement time has been calculated theoretically and numerically for all important parameter regimes, and confirmed experimentally. A typical reactor calculation gives  $Q_E = 2$  for a 400 meter system with 3000 MW(e) output.

The main concern of a multiple-mirror system is stability. Linked quadrupoles can achieve average minimum-B stabilization of flute modes, and experiments have demonstrated this stabilization. Localized instabilities at finite  $\beta$  and enhanced diffusion resulting from the distorted flux surfaces and possibly from turbulent higher order modes still remain to be investigated.

## ACKNOWLEDGEMENT

The authors acknowledge the contributions to the experimental program of Dr. I. Brown, Dr. S. Eylon, J. Riordan, and M. Tuszewski. Helpful discussions with Drs. H. Berk, C. Hartman, and B. McNamara, are gratefully acknowledged. The research was partially supported by ERDA Contract AT(04-3)-34 PA215 and by National Science Foundation Grant ENG 75-02709.

## REFERENCES

1. B. G. Logan, A. J. Lichtenberg, M. A. Lieberman and A. Makhijani, Phys. Rev. Lett. 28 144 (1972).
2. J. B. Taylor, "Multiple Mirrors and R. F. Stoppers," in Culham Laboratory Report CLM-R94, p. 27, U.K.A.E.A., England (1969).
3. G. I. Budker, V. V. Mirnov and D. D. Ryutov, ZHETF Pis. Red. 14 320 (1971).
4. V. V. Mirnov and D. D. Ryutov, Nuclear Fusion 12 627 (1972).
5. B. G. Logan, I. G. Brown, M. A. Lieberman and A. J. Lichtenberg, Phys. Rev. Lett. 29 1439 (1972).
6. A. Makhijani, A. J. Lichtenberg, M. A. Lieberman, B. Grant Logan, Phys. of Fluids 17 1291 (1974).
7. B. G. Logan, I. G. Brown, M. A. Lieberman and A. J. Lichtenberg, Phys. of Fluids 17 1302 (1974).
8. G. I. Budker, V. V. Danilov, E. P. Kruglyakov, D. D. Ryntov, Ye. V. Shun'ko, "Experiments in Confining a Plasma in a Multi-mirror Magnetic Trap," MATT-Trans 108, Princeton Plasma Phys. Lab. (1973).
9. G. I. Budker, "Thermonuclear Fusion in Installations with a Dense Plasma", 6th European Conf. on Plasma Phys. and Contr. Nuc. Fus.
10. J. L. Tuck, Phys. Rev. Lett. 20 715 (1968).
11. A. J. Lichtenberg, "Phase Space Dynamics of Particles", J. Wiley (1969), Sec. 5.5.
12. S. T. Young and M. A. Lieberman, Bul. Am. Phys. Soc. 19 878 (1974).
13. H. P. Furth, J. Killeen, M. N. Rosenbluth, and B. Copi, Proc. Culham Conf. on Plasma Phys. and Contr. Nuclear Fus. Res., 1 103 (1965).
14. A. J. Lichtenberg and B. Myers, Bul. Am. Phys. Soc., 17 1058 (1972).

15. T. Young, J. Benford and S. Putnam, Bull. Am. Phys. Soc. 19, 901 (1974).
16. F. L. Ribe, "Fusion Reactor Systems", Los Alamos Scientific Laboratory Report LA-UR-74-758.
17. H. P. Furth and M. N. Rosenbluth, Phys. Fluids 7 764 (1964).
18. B. Grant Logan, "Current-Stabilization of the Curvature Driven M = 1 Mode", Lawrence Livermore Laboratory, Report UCID 16615 (1974).
19. R. W. Moyer, Ed., Committee Report: Lawrence Livermore Laboratory Re-evaluation of the Simple Mirror for a Fusion Reactor, App. D. UCID-16736 (1975).
20. N. Lindgren and C. K. Birdsall, "Feedback Suppression of Collisionless Multimode Drift Waves in a Mirror-Confined Plasma", Phys. Rev. Lett. 24 1159 (1970).

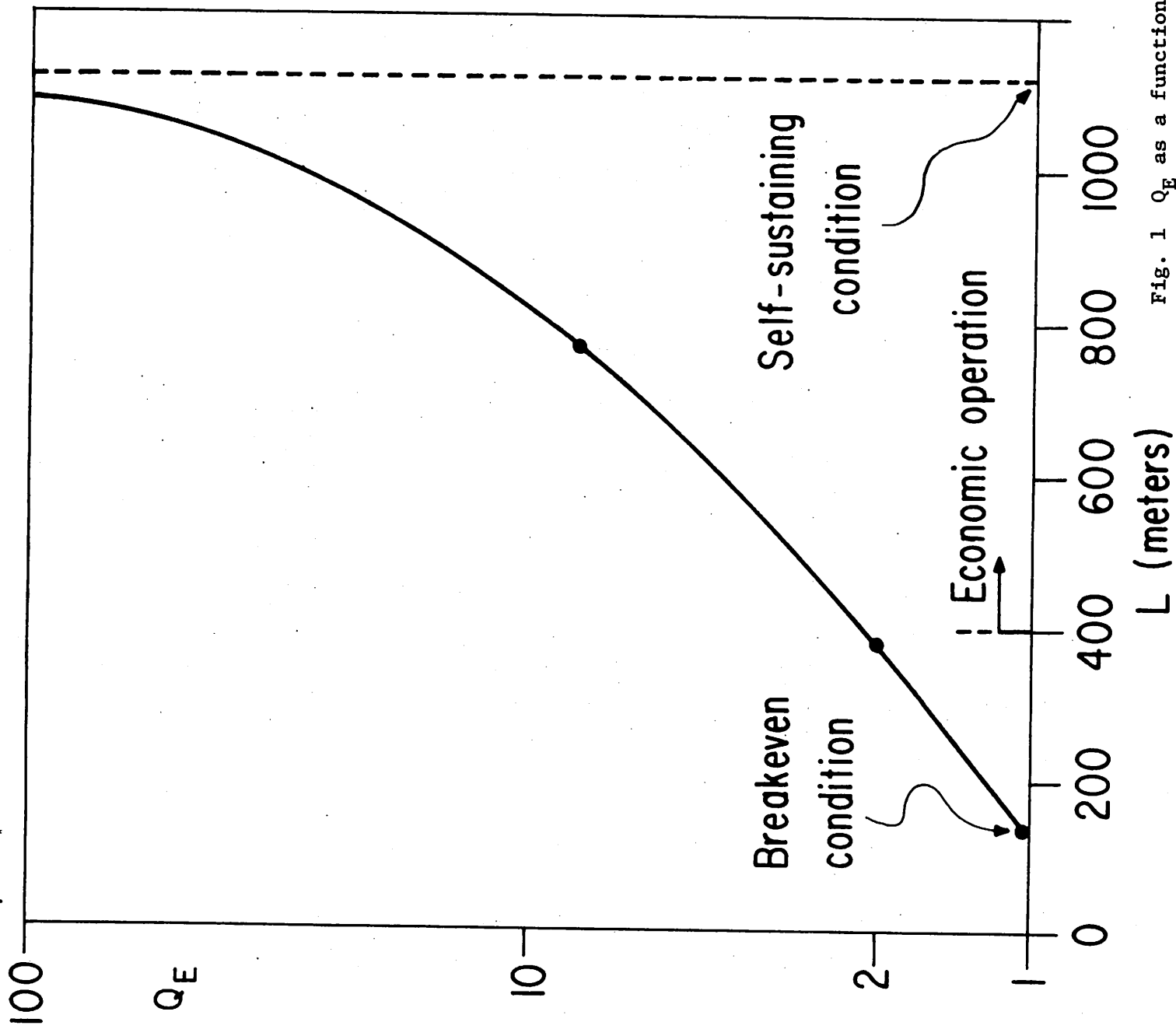
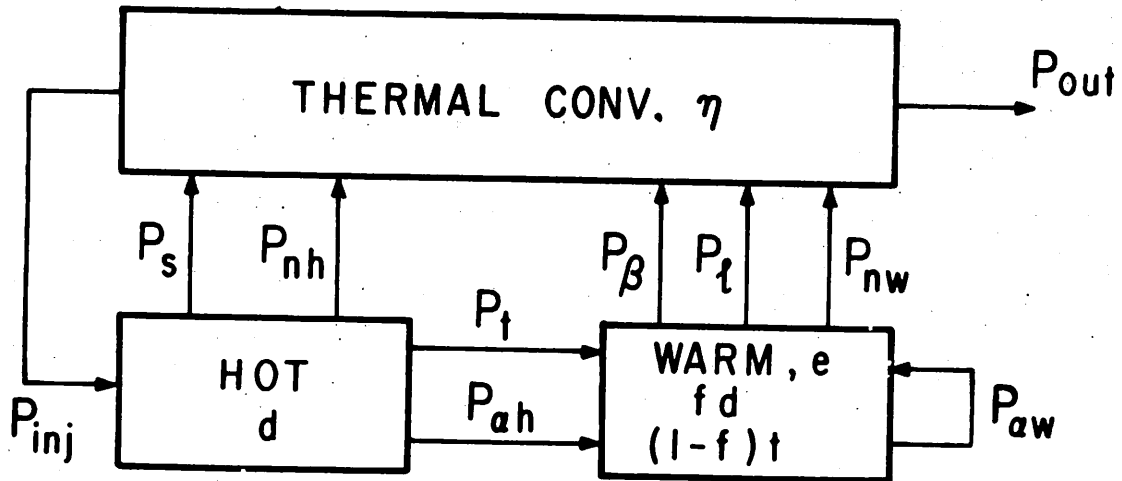


Fig. 1  $Q_E$  as a function of total length  $L$ .

# POWER FLOWS IN TWO-COMPONENT MULTIPLE MIRROR



$$\epsilon = n_h / n_e, \quad f = n_d / (n_d + n_t), \quad P_t \propto \frac{T^{7/2}}{M^2 L^2}$$

Fig. 2 Schematic of power flows

# MULTIPLE MIRROR (Q=3)

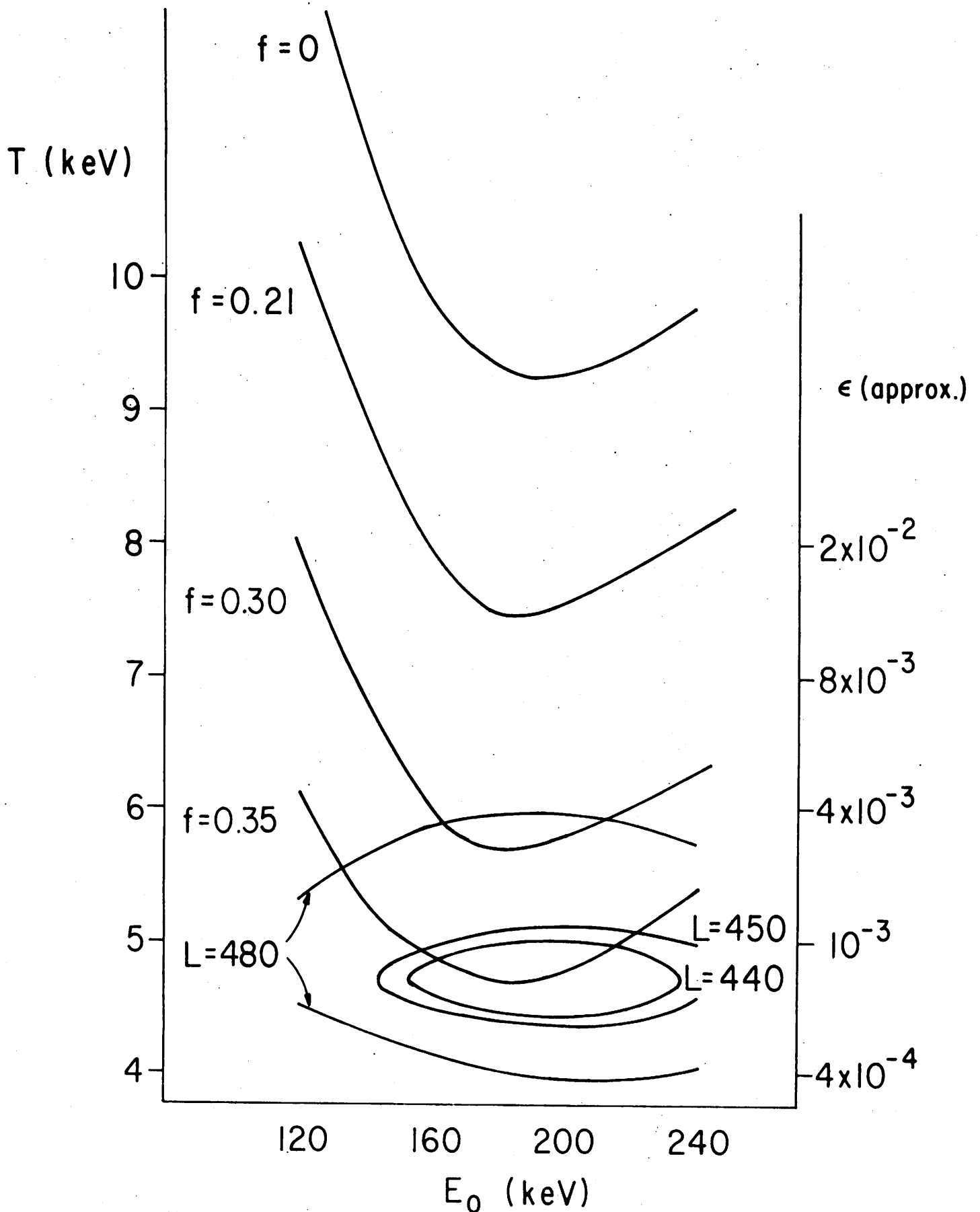


Fig. 3 Optimization of a two component multiple-mirror reactor

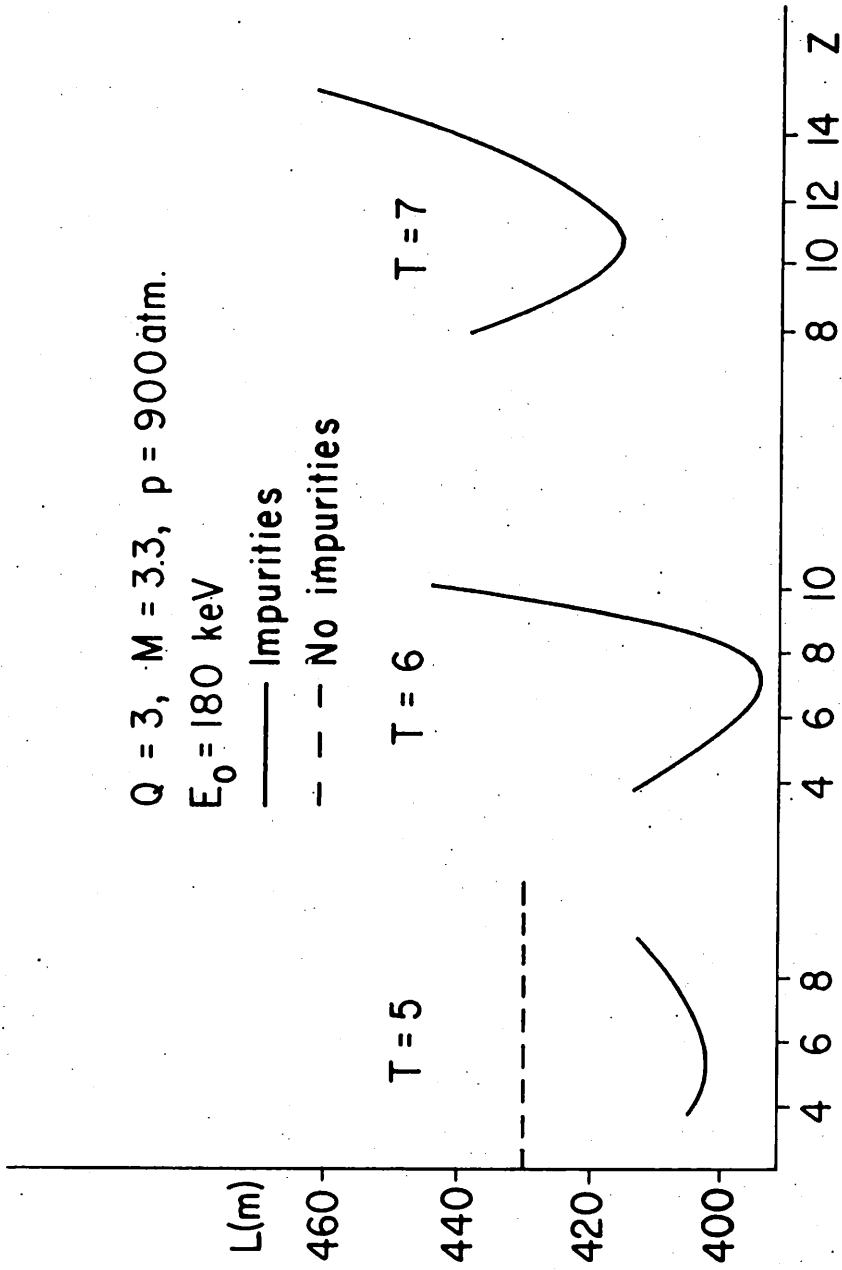


Fig. 4 Minimization of the length of a multiple-mirror reactor by impurity seeding



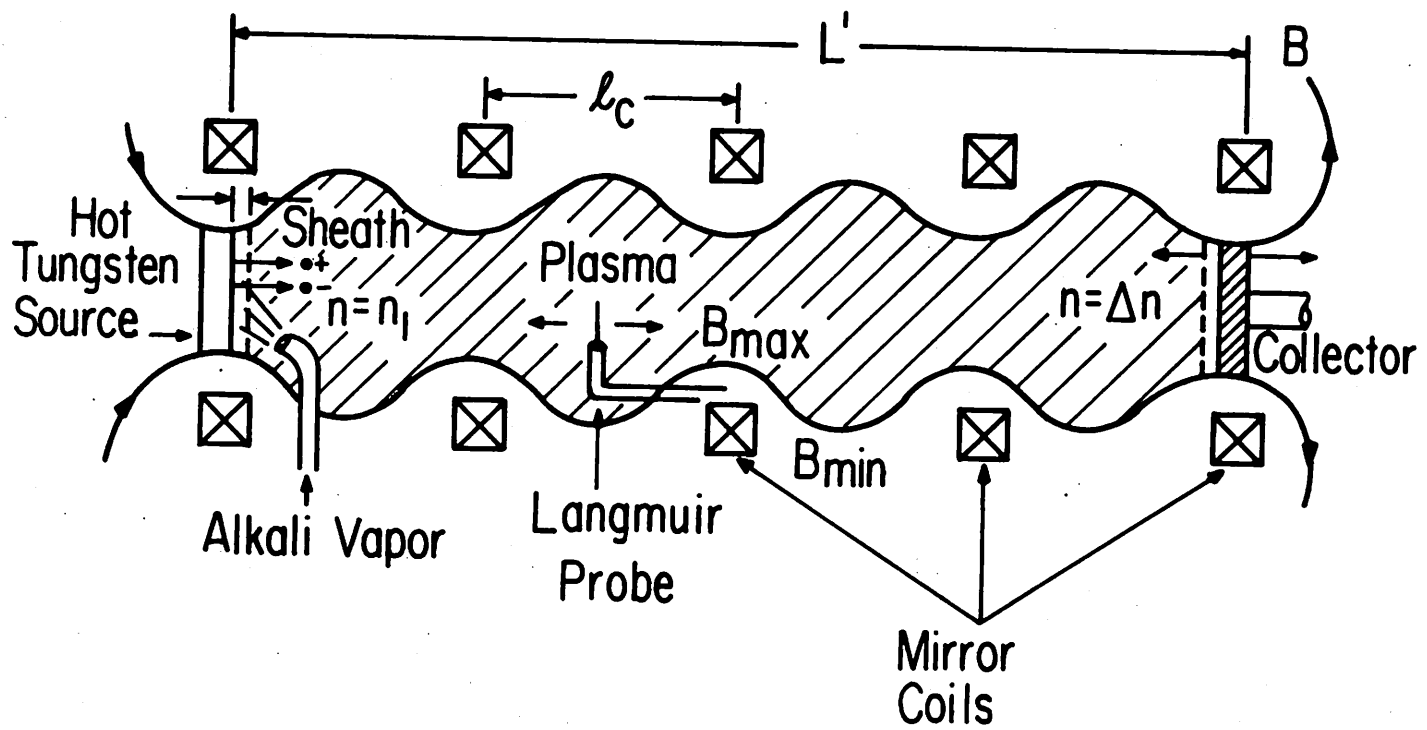


Fig. 5 The Multiple-Mirror Experiment

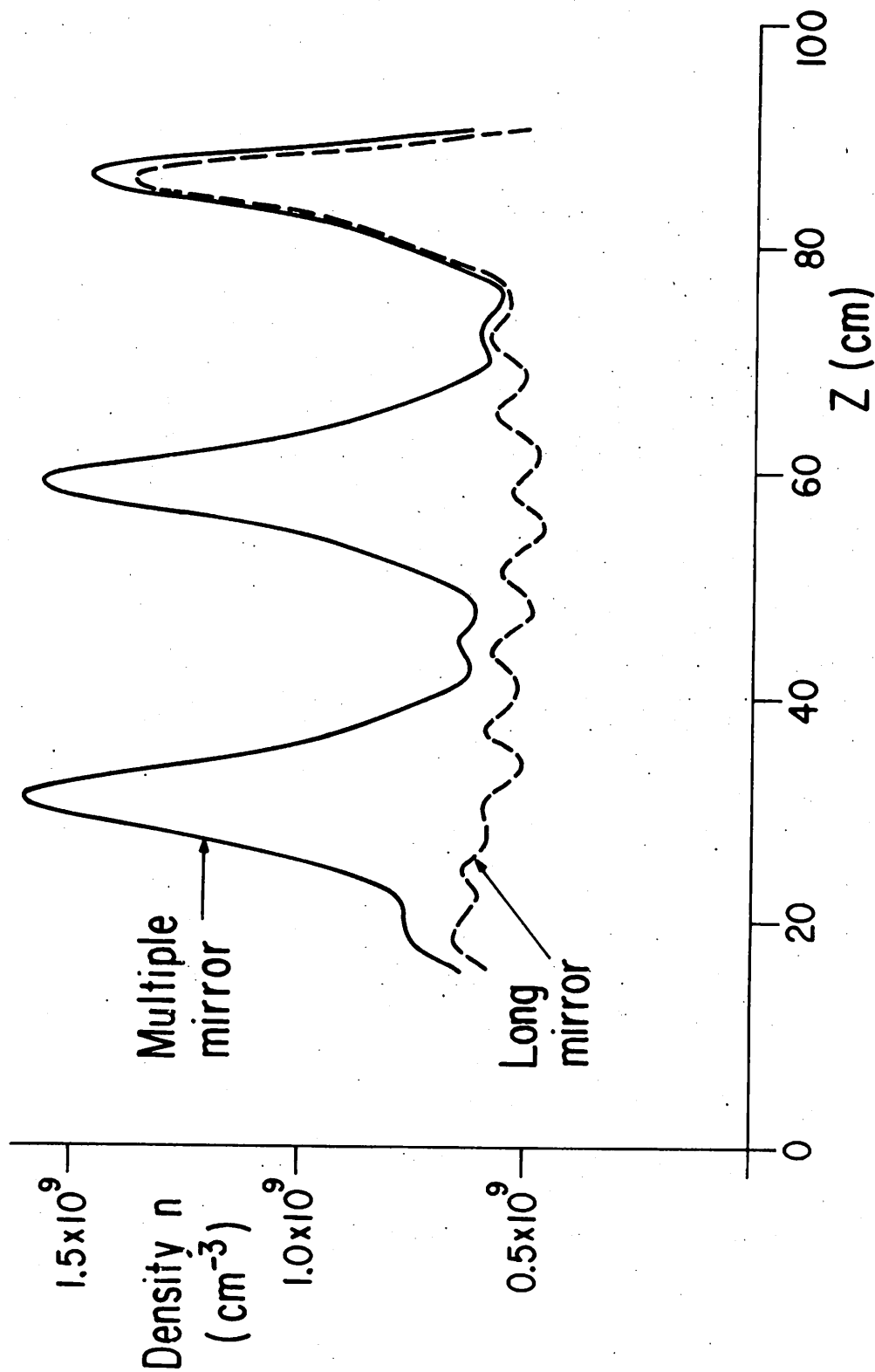


Fig. 6a. 3 cell (solid line) and long mirror (dashed line) density as a function of  $z$  for the low density regime. Potassium.

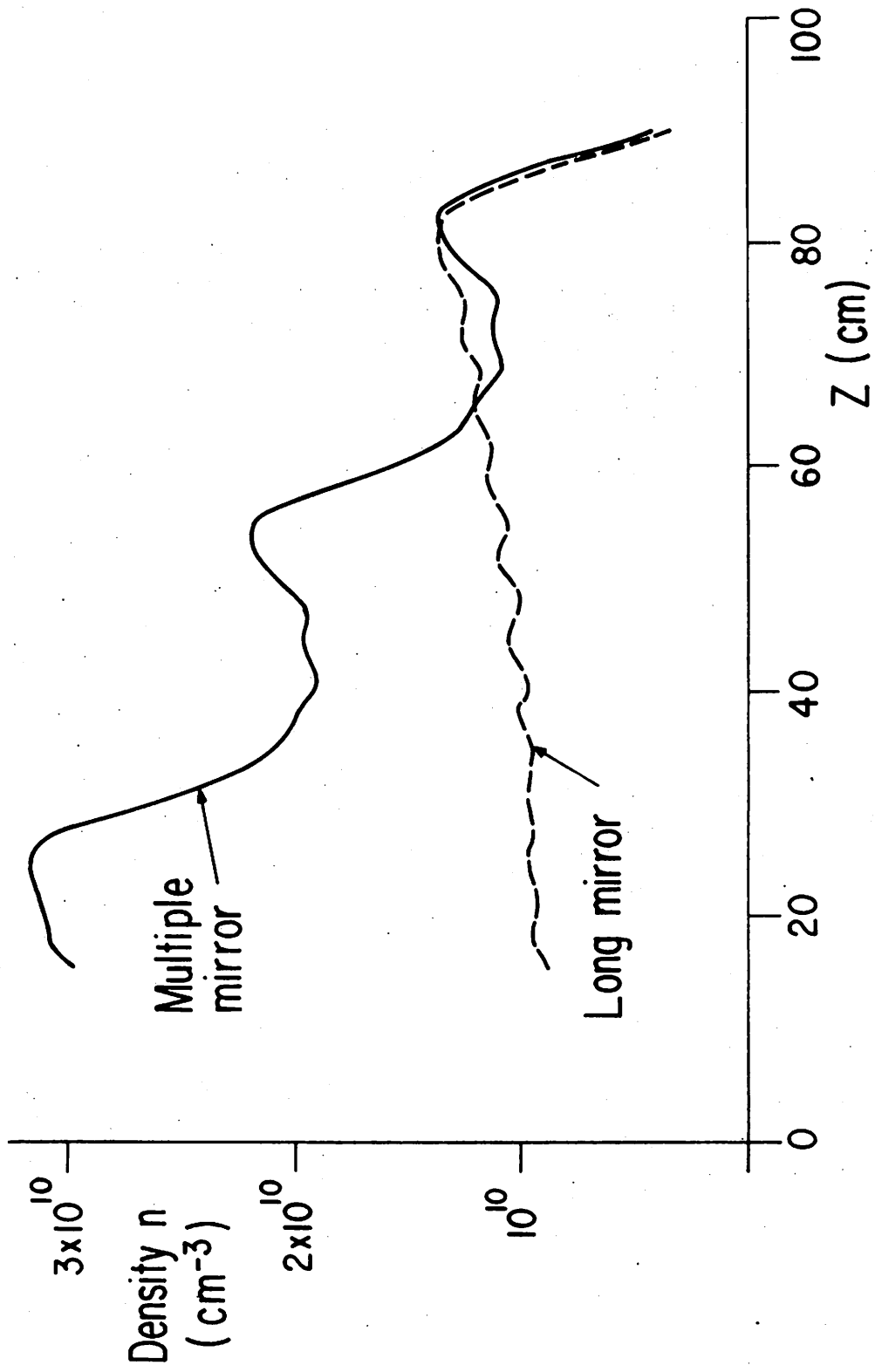


Fig. 6b 3 cell (solid line) and long mirror (dashed line) density as a function of  $z$  for the intermediate density regime.

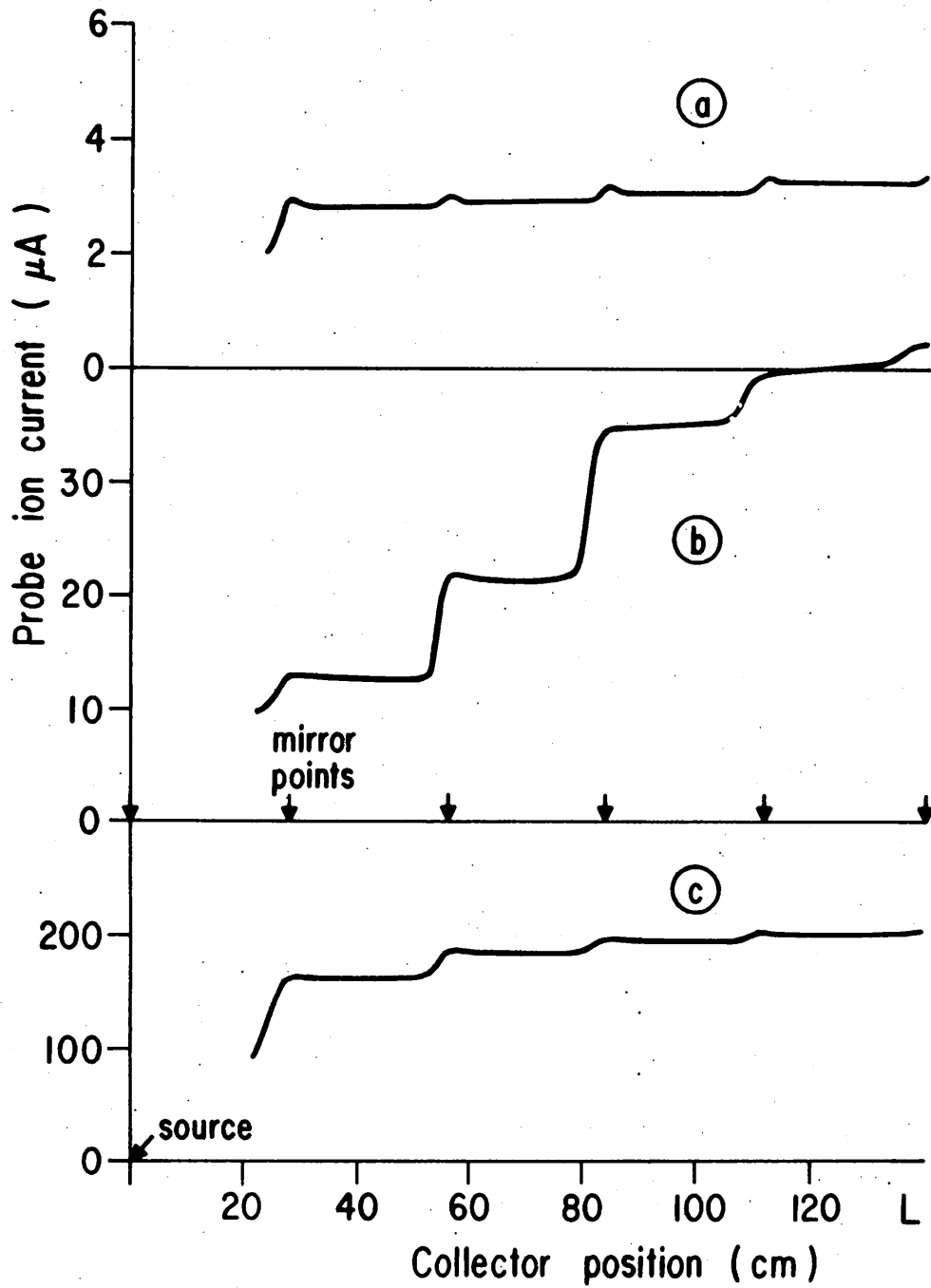


Fig. 7 Langmuir probe ion saturation current (density  $n_1$ ) in the first cell as a function of collector position, in the (a) low density, (b) intermediate density, and (c) high density regimes. Potassium, 5 cells

Field Line For Partially Compensated Field

Mirror Ratio = 2.5

$i_Q = .3$     $i_A = .2$

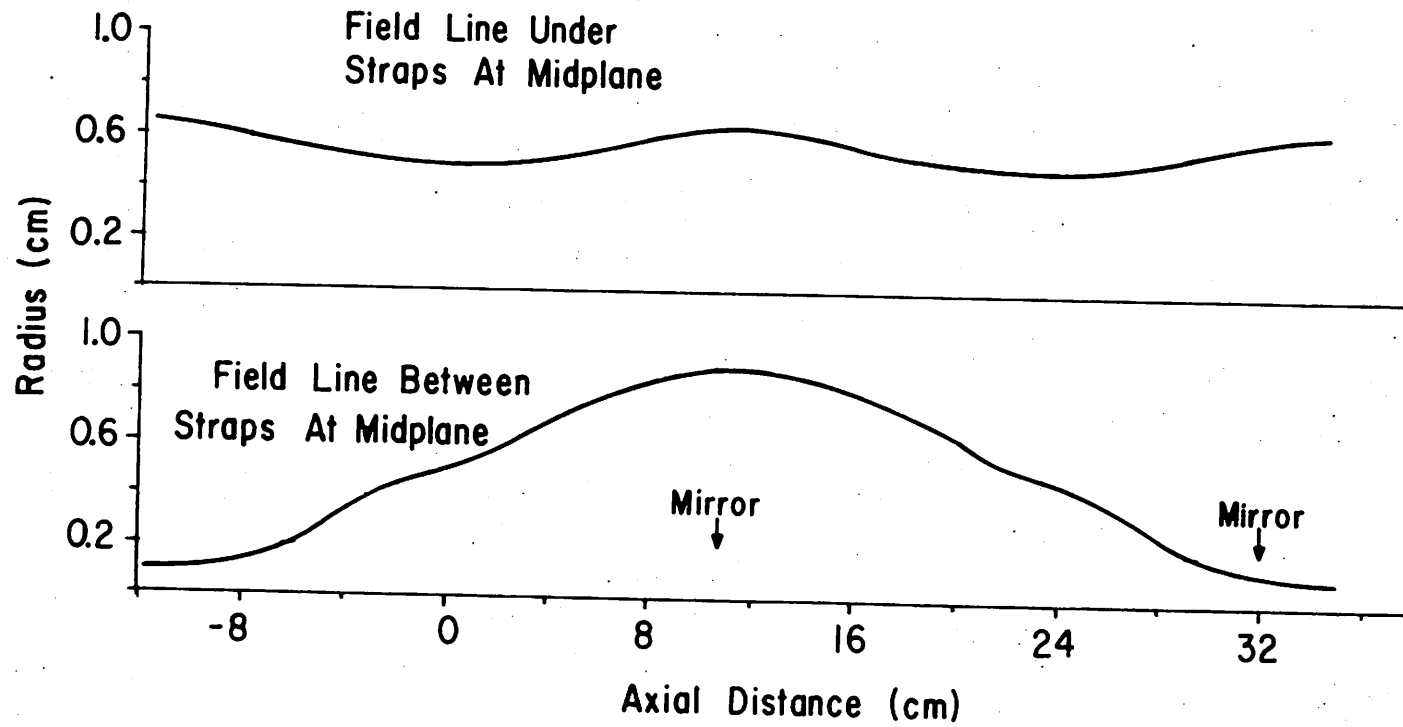
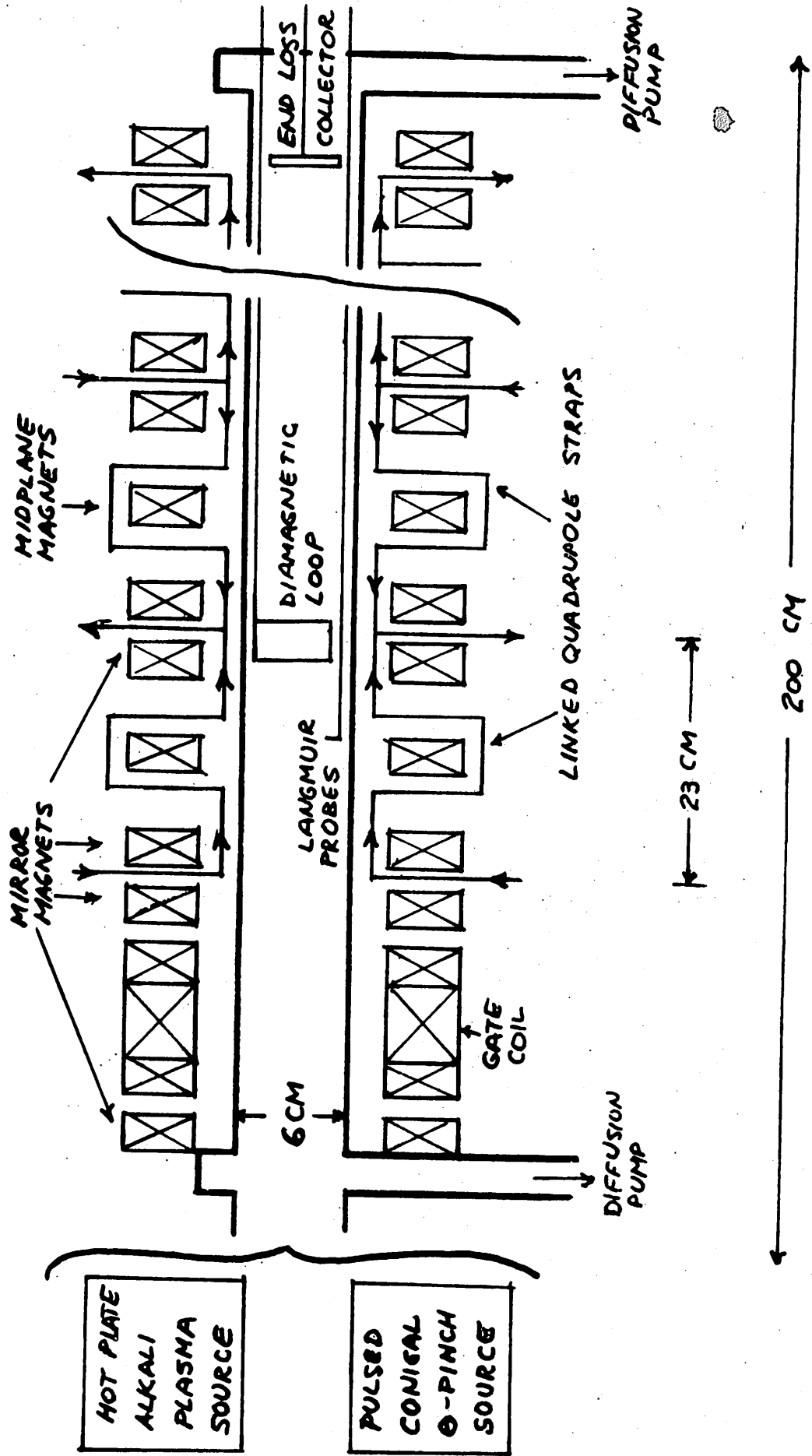


Fig. 8 Characteristic field lines for quadrupole field at which best compensation was achieved.

Fig. 9 Schematic of multiple-mirror device including quadrupole windings.

# 7 CELL MULTIPLE MIRROR / LINKED QUADRUPOLE SYSTEM



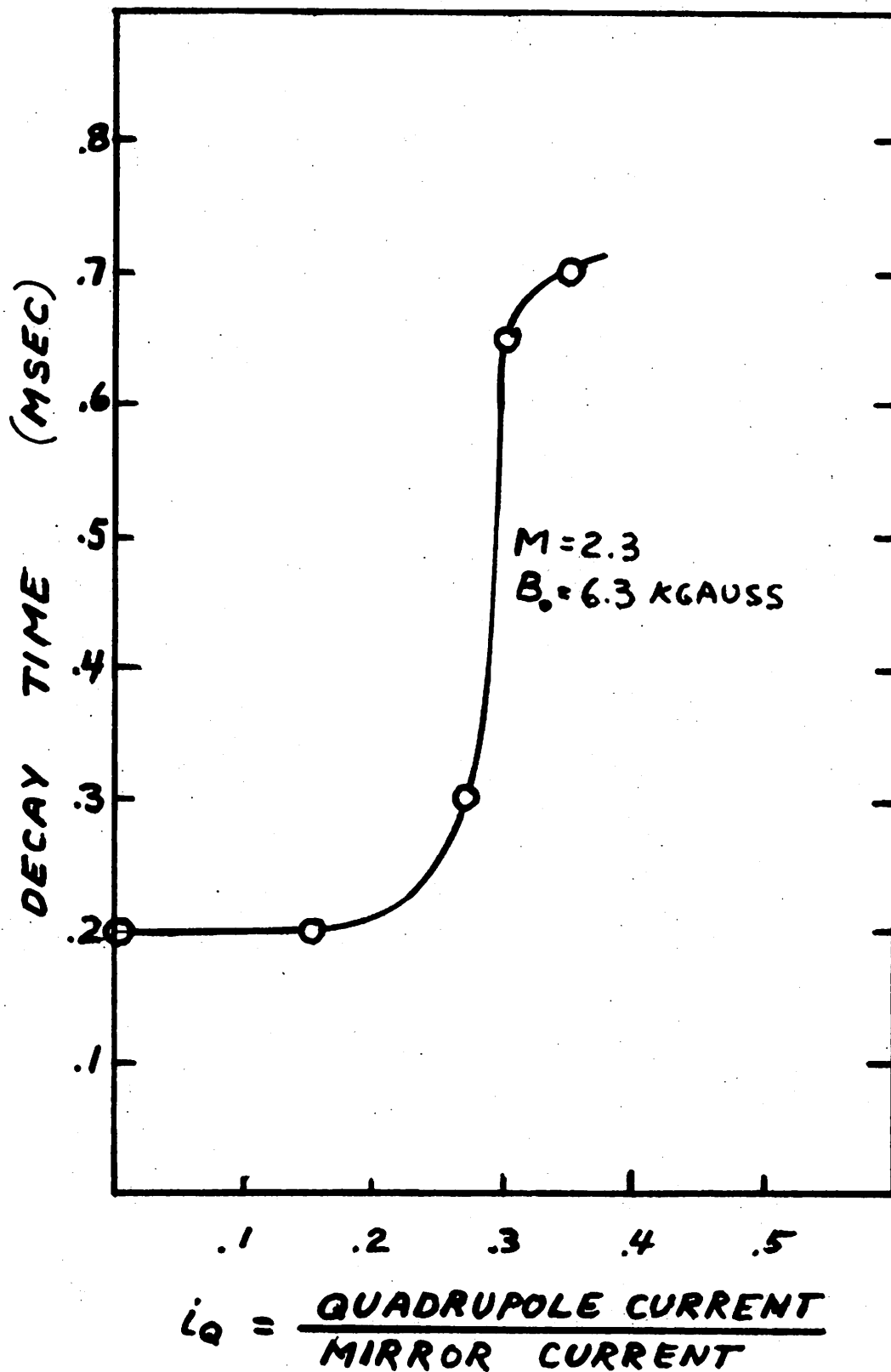


Fig. 10 Stabilization of multiple-mirror confined plasma with increasing quadrupole field (contact ionization source)

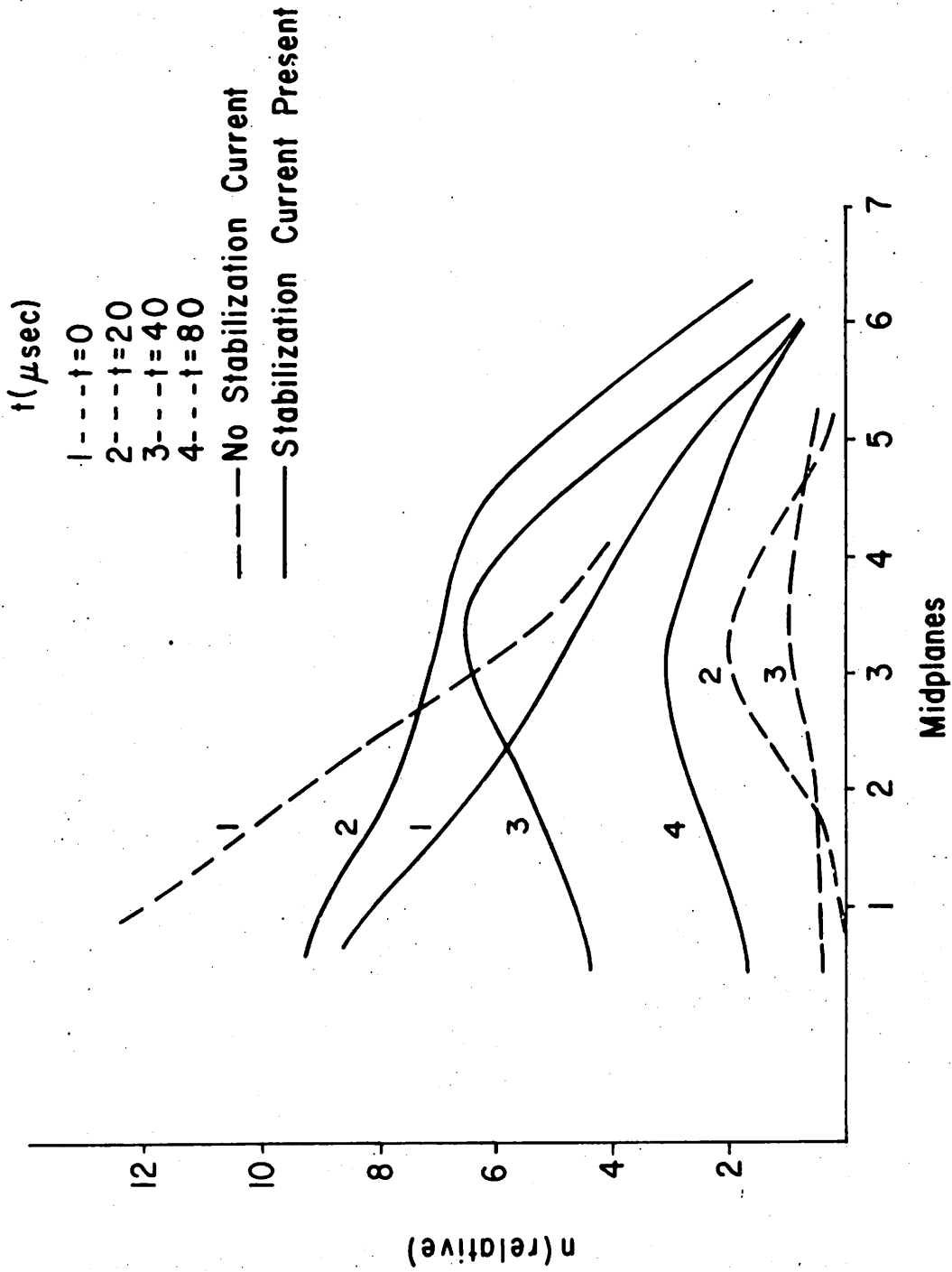


Fig. 11 Decay of axial density in multiple mirror with and without stabilization  
( $\theta$ -pinch plasma source)